MR perfusion imaging by alternate slab width inversion recovery arterial spin labeling (AIRASL): a technique with higher signal-to-noise ratio at 3.0 T

doi: 10.1007/s10334-011-0301-8

Original Research

MR perfusion imaging by alternate slab width inversion recovery arterial spin labeling (AIRASL): a technique with higher signal-to-noise ratio at 3.0 T

Yasuhiro Fujiwara, MS[1,2]; Hirohiko Kimura, MD, PhD[3]; Tosiaki Miyati, PhD, MDSc[2]; Hiroyuki Kabasawa, PhD[4]; Tsuyoshi Matsuda, RT[5]; Yoshiyuki Ishimori, PhD[6]; Isao Yamaguchi, PhD[7]; Toshiki Adachi, MS[1]

1) Radiological Center, University of Fukui Hospital, 2) Division of Health Sciences, Kanazawa University Graduate School of Medical Science, 3) Departments of Radiology, University of Fukui, 4) Applied Science Laboratory Japan, GE Healthcare Japan Corporation, 5) Advanced Application Center, GE Healthcare Japan Corporation, 6) Department of Radiological Sciences, Ibaraki Prefectural University of Health Sciences, 7) Department of Radiological Technology, Osaka Butsuryo College

Correspondence should be addressed to **Hirohiko Kimura, MD, PhD**
Department of Radiology, University of Fukui,
23-3 Matsuoka-shimoaizuki, Eiheiji-cho, Yoshida-gun, Fukui 910-1193, Japan
Phone: +81-776-61-8371; Fax: +81-776-61-8137, E-mail: kimura@u-fukui.ac.jp

Abstract 216word, text 3543 words, 7figures, 1table, and 18references

Abstract

Object: To propose a new arterial spin labeling (ASL) perfusion-imaging method (alternate slab width inversion recovery ASL: AIRASL) that takes advantage of the qualities of 3.0T.

Materials and Methods: AIRASL utilizes alternate slab width IR pulses for labeling blood to obtain a higher signal-to-noise ratio (SNR). Numerical simulations were used to evaluate perfusion signals. In vivo studies were performed to show the feasibility of AIRASL on five healthy subjects. We performed a statistical analysis of the differences in perfusion SNR measurements between flow–sensitive alternating inversion recovery (FAIR) and AIRASL.

Results: In signal simulation, the signal obtained by AIRASL at 3.0T and 1.5T was 1.14% and 0.85%, respectively, whereas the signal obtained by FAIR at 3.0T and 1.5T was 0.57% and 0.47%, respectively. In an in vivo study, the SNR of FAIR (3.0T) and FAIR (1.5T) were 1.73 ± 0.49 and 1.02 ± 0.20, respectively, whereas the SNRs of AIRASL (3.0T) and AIRASL (1.5T) were 3.93 ± 1.65 and 1.34 ± 0.31, respectively. SNR in AIRASL at 3.0T was significantly greater than that in FAIR at 3.0T.

Conclusion: The most significant potential advantage of AIRASL is its high SNR, which takes advantage of the qualities of 3.0T. This sequence can be easily applied in the clinical setting and will enable ASL to become more relevant for clinical application.

Key Words: Arterial spin labeling, Magnetic resonance imaging, High field, Perfusion

Introduction

Arterial spin labeling (ASL) methods allow repeated noninvasive determination of cerebral blood flow (CBF). ASL has been used in numerous applications, ranging from basic neuroscience using animal models and human volunteers to clinical perfusion measurement [1-7]. ASL techniques can be classified as continuous or pulsed arterial spin labeling (CASL or PASL, respectively). Because the PASL approach is undemanding in terms of hardware performance (RF deposition limits) compared with CASL, PASL is easier to implement in clinical magnetic resonance (MR) systems. During the past decade, methodologies for PASL perfusion MR imaging have evolved from feasibility studies into the practical use stage. A weakness of the technique, however, is its low signal-to-noise ratio (SNR), which is caused by the small fractional effect of the labeled blood (<1% raw signal) and by T1 decay of the labeled arterial blood magnetization during transit from the tagging location to the tissue. As a result, there are few reports regarding the clinical application of PASL.

The recent development of high-field ASL at 3.0T enables increased SNR that is proportional to the main field strength. This provides an important advantage for labeling; because of the increase in relaxation time T1 with the high field, the loss of spin labeling during the transit time is decreased, and accumulation of labeled spins is increased over that at 1.5T, producing greater perfusion signals in brain tissue while reducing the arterial transit-related artifacts and quantification errors. Therefore, the move to 3.0T high-field

scanners in standard clinical environments facilitates the progression of this method from the research and development stage towards clinical applications. Consequently, development of a new pulse sequence that makes full use of the characteristics of the high field is required for clinical MR systems.

The purpose of this study was to propose a new pulse sequence (alternate slab width inversion recovery ASL: AIRASL) that takes advantage of the qualities of 3.0T. AIRASL utilizes alternate slab width inversion pulses for labeling blood to obtain a higher SNR. We evaluated the feasibility and performance of AIRASL for perfusion measurements and performed a statistical analysis of the difference in perfusion SNR measurements between flow–sensitive alternating inversion recovery (FAIR) and AIRASL.

Theory

The AIRASL sequence uses multiple narrow and wide spatially selective inversion recovery (IR) pulses to label the longitudinal magnetization of protons in the blood (Fig. 1, 2).

In the first labeling period, a spatially selective IR pulse is applied to a narrow slab just slightly larger than the imaging volume. Immediately after the pulse, the spins within the narrow slab are inverted and uninverted spins from outside the volume begin to flow in. After the first interval IT, a second IR pulse is applied to a wider slab containing the narrow slab. The slab of tissue beneath the narrow slab but within the wider slab will be referred to as the

labeling slab (Fig. 2). Immediately after the second IR pulse, the spins in the vasculature located within the labeling slab are inverted, whereas spins in the imaging region revert to their original orientation. After a second interval IT, a third pulse is applied to the narrow slab in a manner similar to the first IR pulse.

In each inversion period, the orientation of inflowing spins tends to be opposite to the orientation in the imaging volume (Fig. 3a). Therefore, an intermittent bolus of labeled spins will flow into the narrow slab, where the imaging is performed. Although this concept of a train of inversion pulses producing a continuous-like ASL effect is similar to that described in a previous report [8], an AIRASL pulse sequence was not used in that study.

The required control scan is acquired using IR pulses with narrow selective pulses replaced with wider selective pulses and vice versa. In this control scan, inflowing spins tend to retain the same orientation as in the imaged volume (Fig. 3b). Perfusion-weighted images can be obtained by subtracting the control image from the labeled image.

Single Compartment Model

Perfusion signal was simulated using the single compartment model, which is described by the modified Bloch equation. The rate of change in longitudinal magnetization, *M*, in the tissue voxel can be described as:

$$\frac{dM(t)}{dt} = -\frac{M_0 - M(t)}{T_1} + fM_a(t) - \frac{f}{\lambda}M(t), \quad [1]$$

where M_0 is the longitudinal equilibrium magnetization of tissue, M_a is the longitudinal magnetization of the arterial blood, T_1 is the longitudinal relaxation time of tissue, f is the cerebral blood flow (ml/100g/min), and λ is the brain–blood partition coefficient of water, which is assumed in this study to have a constant value of 0.9 ml/g [9]. For a full definition of the parameters, see Table 1.

Modeling of ASL signal for different ratios of slab width to flow velocity is very complicated. However, the most efficient labeling will tend to occur when the time for blood to cross the slab (labeling slab width / flow velocity) is equal to the time between inversions (IT). For the analysis in this work, we will assume this relationship recognizing that this will not be perfectly achieved in vivo and thus flow will tend to be underestimated. Under this assumption, the equation solutions are summarized in Eqs. 2, 3 and 4 as follows (see Appendix):

$$\Delta S_1(t) = e^{-\frac{t-\delta_a}{T_{1app}}}\left[\frac{2\alpha f M_0}{\lambda}\cdot e^{-\frac{\delta_a}{T_{1a}}}\cdot\frac{1}{\frac{1}{T_{1app}}-\frac{1}{T_{1a}}}\cdot e^{\left(\frac{1}{T_{1app}}-\frac{1}{T_{1a}}\right)(t-\delta_a)} - \frac{2\alpha f M_0}{\lambda}\cdot e^{-\frac{\delta_a}{T_{1a}}}\cdot\frac{1}{\frac{1}{T_{1app}}-\frac{1}{T_{1a}}}\right]$$

$$(\delta_a < t \le IT). \qquad [2]$$

$$\Delta S_1(0) = 0 \qquad (0 < t \le \delta_a). \qquad [3]$$

Where $\Delta S_1(t)$ represents ASL signal in the 1st period.

$$\Delta S_i(t) = e^{-\frac{(t-\delta_a-(i-1)*IT)}{T_{1app}}}\left[\frac{2\alpha f M_0}{\lambda}\cdot e^{-\frac{\delta_a}{T_{1a}}}\cdot\frac{1}{\frac{1}{T_{1app}}-\frac{1}{T_{1a}}}\cdot e^{\left(\frac{1}{T_{1app}}-\frac{1}{T_{1a}}\right)(t-\delta_a-(i-1)*IT)}\right.$$

$$\left. + S_{i-1}\left((i-1)*IT+\delta_a\right) - \frac{2\alpha f M_0}{\lambda}\cdot e^{-\frac{\delta_a}{T_{1a}}}\cdot\frac{1}{\frac{1}{T_{1app}}-\frac{1}{T_{1a}}}\right] \quad (\delta_a < t). [4]$$

where $\Delta S_i(t)$ represents the difference in magnetization between the control and labeled images from the i-1 to i-th pulse period where 1<i, M_0 is the equilibrium value of magnetization, δ_a is the transit time between the labeling and imaging planes, T_{1app} and T_{1a} are the apparent longitudinal relaxation times of brain tissue and blood, f is blood flow, IT is the time between IR pulses and i is the number of the IR pulses in the sequence.

Materials and Methods

Numerical Simulation

We first used a numerical simulation to evaluate perfusion signal using Eqs. 2, 3 and 4 with the following parameters: IT = 600 ms. We calculated the perfusion signals of FAIR and AIRASL at 1.5T and 3.0T.

Second, we calculated the perfusion signal of AIRASL with the time between IR pulses from 300 to 1200 ms at a blood flow velocity of 20 cm/s at 3.0T, respectively, in order to determine the optimal time between IR pulses. Because our simulations assume that the labeling slab width / flow velocity is equal to IT, these simulations for different IT should be considered as each having the slab width adjusted to meet this condition for the particular IT.

In Vivo Measurements

In vivo studies were performed to show the feasibility of AIRASL on human subjects and to verify consistency between the efficacy of the technique in vivo and the simulation results. Five healthy volunteers (five males, 27–30 years old) gave written informed consent before scanning, and all protocols were approved by our Institutional Review Board.

AIRASL and FAIR were obtained in subjects using 1.5T and 3.0T MR systems (Signa Excite HD, GE Medical Systems, Milwaukee, MI), using an eight-channel phased array head coil. AIRASL imaging was performed using a single shot echo planar sequence with the following parameters: field of view (FOV) = 240 × 240 mm; slice thickness = 6 mm; slice gap = 1 mm; number of slices = 7; repetition time (TR) = 4000 ms; echo time (TE) = 18.8 ms; matrix size = 128 × 128; scan time = 4 min; ASSET factor of parallel imaging = 2; narrow and wide spatially selective IR pulse tagging with tag thicknesses of 63.7 and 163.7 mm using hyperbolic secant adiabatic pulses; effective width of tagging slab = 50 mm; time between IR pulses (interval time: IT) = 600 ms; time between third IR and acquisition (post-labeling delay time) = 1400 ms. Conventional FAIR imaging used the same imaging parameters and times as that for AIRASL imaging, with the exception of interval time. The inversion time of FAIR imaging was 1400 ms.

Perfusion weighted images were calculated by pair-wise subtraction of the control and label

images followed by averaging across the image series using an in-house program written using an IDL software system (ITT Visual Information Solutions, Boulder, CO).

Image Analysis

We measured the SNR of AIRASL and FAIR to evaluate the efficacy of spin labeling of blood in an in vivo study. SNR was calculated by dividing the average signal in the region of interest (ROI) within the brain by the standard deviation of noise in perfusion images. The foreground ROI covered the cortex of the middle cerebral artery territory in a section of the centrum semiovale. Noise was defined as the standard deviation in the region of the anterior horn of the lateral ventricle.

A paired-*t* test was used to compare each method and magnetic field in normal volunteers. A two-sided P value of less than 0.05 was considered to indicate statistical significance.

Results

Numerical Simulation

We simulated perfusion signals obtained by AIRASL and FAIR at 3.0T and 1.5T. Figure 4 shows the dynamics of labeled arterial spin signal, showing the passage of labeled spins through the microvasculature at 1.5T and 3.0T. The signal obtained by AIRASL at 3.0T and 1.5T was 1.14% and 0.85%, respectively, whereas the signal obtained by FAIR at 3.0T and

1.5T was 0.57% and 0.47%, respectively. The signal of obtained with AIRASL at 3.0T was double of that of FAIR at 3.0T. Figure 5 demonstrates the relationship between %signal change of AIRASL and the time between IR pulses. We decided to employ a time between IR pulses of 600ms because the optimal signal per square root of imaging time is obtained with IT in the 600-1200ms range (Fig 5).

In Vivo Analysis

Perfusion images obtained by AIRASL and FAIR at 1.5T and 3.0T are shown in Figure 6. SNR in the territory of the middle cerebral artery obtained by AIFAR and FAIR are shown in Fig. 7. The SNR of FAIR (3.0T) and FAIR (1.5T) were 1.73 ± 0.49 and 1.02 ± 0.20, respectively, whereas the SNRs of AIRASL (3.0T) and AIRASL (1.5T) were 3.93 ± 1.65 and 1.34 ± 0.31, respectively. At 1.5T, there was no significant difference in SNR between AIRASL and FAIR. At 3.0T, SNR in AIRASL was significantly better than that in FAIR ($P < 0.01$). Moreover, SNR in AIRASL was significantly better at 3.0T than at 1.5T ($P < 0.01$).

Discussion

The present study demonstrates the feasibility and advantages of acquiring ASL perfusion images using the AIRASL sequence at 3.0T.

The results of signal simulation for FAIR showed that the perfusion signal obtained by FAIR

was 0.57% and 0.47% at 3.0T and 1.5T, respectively. The perfusion signal obtained by FAIR only increased by a factor of 1.21 with an increased magnetic field strength at 3.0T. This finding indicates that it is difficult to obtain a large increase in SNR by increasing field strength alone. Therefore, while 3.0T MRI has been widely adopted, the clinical applications of FAIR remain limited. On visual inspection, the FAIR perfusion images obtained at 3.0T in the present in vivo study showed little improvement on those acquired at 1.5T.

In contrast, the results of signal simulation for AIRASL revealed perfusion signals of 1.14% and 0.85% at 3.0T and 1.5T, respectively. The SNR of the perfusion signal obtained in AIRASL was 2.27 (3.93/1.73) and 1.31 (1.34/1.02) times higher at 3.0T and 1.5T, respectively, than that obtained in FAIR. In AIRASL, the inflowing blood spins are intermittently labeled using multiple IR pulses. Therefore, when compared with FAIR, AIRASL enables more labeled spins to flow into static tissue in a single acquisition. The results of our in vivo study showed that both magnetic field strengths yielded a marked improvement in SNR in the perfusion images obtained using AIRASL, compared with those using FAIR.

In the technique of pulsed arterial spin labeling, high-field MRI is appealing because it provides increased SNR, as well as advantages in labeling because of the increased relaxation time T1 of labeled blood. Signal simulation revealed that perfusion signals obtained using AIRASL showed a similar increase at both magnetic field strengths, compared with that obtained using FAIR. The improvement of SNR in the in vivo study for AIRASL at 3.0T

approximated that of the signal simulation. In contrast, due to the limitations of SNR and short T1 value of labeled blood at 1.5T, there was only limited improvement in the SNR when using AIRASL at 1.5T.

Previous studies reported using physiological noise reduction or background suppression because of the low inherent SNR of PASL [10-12]. However, few studies have sought to increase labeling efficiency [13-15].

AIRASL greatly improves image quality, although there are currently a number of drawbacks with this technique. First, because fresh blood spins flow into the imaging slice between the last IR pulse and acquisition, the high signal of the fresh blood spins remains in the imaging slice, and the high signal remaining in vessels may lead to overestimation of perfusion in the gray matter. Strong bipolar crusher gradients may be effective in decreasing vascular signals in the AIRASL sequence [16, 17]. Otherwise, using a longer delay time from the last IR pulse to acquisition may also be effective in decreasing vascular signals in the AIRASL sequence. Since the SNR is greater with AIRASL than with FAIR, AIRASL enables a longer post-labeling delay time from the last IR pulse to acquisition. In addition, by using a prolonged post-labeling delay time, the effect of transit time can be reduced. Because its SNR is high enough, it is possible to decrease the number of averages in AIRASL when compared with FAIR. And also, the FAIR width could be made larger but in many applications, geometry and hardware limit the feasible bolus width. Therefore, AIRASL enables multiple

measurements with different labeling. For example, a perfusion-weighted image can be obtained at multiple delay times to correct for transit time errors or to obtain a T1 map for CBF calculation.

Although the SNR is superior with AIRASL acquisition than with conventional single pulsed FAIR, the quantification of AIRASL signal may be complicated by the uncertainty of the multiple inflow function during label periods. Theoretically, if we obtain the flow velocity of the carotid artery during the label periods, the calculation of blood flow may be possible using Eq. 27. However, for the time being, the qualitative use of AIRASL may be more practical in the clinical setting.

Another problem with AIRASL is that the repeated IR pulses for labeling blood may lead to underestimation of perfusion. In patients with severe obstructive internal carotid artery disease, the presence of collateral blood flow may increase the transit time of the labeled blood flow to the brain tissue. In the case of marked slowing of blood flow velocity, the second IR pulse is applied to the inversion area before blood labeled by the first IR pulse has completely flowed into the imaging slab, thereby enabling labeled blood to be re-inverted. In addition, the third IR pulse is applied to negate signals from blood labeled using the second IR pulse. Therefore, in perfusion studies of disease with long arterial transit time, such as in stroke patients, the time between each RF pulse application to excitation should be considered to avoid loss of the labeling effect. AIRASL will be velocity sensitive, but may be useful in

applications where a good estimate of bolus width is available or when relative blood flow is required. For example, high SNR relative blood flow AIRASL may be highly useful for the purpose of neural activation imaging in a functional MRI study using human volunteers and for clinical perfusion measurements in patients with brain tumors and degenerative brain disease where relative blood flow may be diagnostic.

Conclusion

This study characterized the AIRASL perfusion-imaging sequence at 3.0T and demonstrated that the most significant advantage of AIRASL is its high SNR. This sequence can be easily applied in the clinical setting and will enable ASL to become more relevant for clinical application.

References

1. Chalela JA, Alsop DC, Gonzalez-Atavales JB et al (2000) Magnetic resonance perfusion imaging in acute ischemic stroke using continuous arterial spin labeling. Stroke 31 (3):680-687.

2. Chen J, Licht DJ, Smith SE et al (2009) Arterial spin labeling perfusion MRI in pediatric arterial ischemic stroke: initial experiences. J Magn Reson Imaging 29 (2):282-290.

3. Garcia DM, Duhamel G, Alsop DC. (2004) The efficiency of background suppression in arterial spin labeling. AlternateProceedings of the 12 th Annual Meeting of ISMRM, kyoto:1360.

4. Herscovitch P, Raichle ME (1985) What is the correct value for the brain--blood partition coefficient for water? J Cereb Blood Flow Metab 5 (1):65-69.

5. Kim MJ, Kim HS, Kim JH et al. (2008) Diagnostic accuracy and interobserver variability of pulsed arterial spin labeling for glioma grading. Acta Radiol 49 (4):450-457.

6. Kimura H, Kado H, Koshimoto Y et al. (2005) Multislice continuous arterial spin-labeled perfusion MRI in patients with chronic occlusive cerebrovascular disease: a correlative study with CO2 PET validation. J Magn Reson Imaging 22 (2):189-198.

7. Kimura H, Takeuchi H, Koshimoto Y et al (2006) Perfusion imaging of meningioma by using continuous arterial spin-labeling: comparison with dynamic susceptibility-weighted contrast-enhanced MR images and histopathologic features. AJNR Am J Neuroradiol 27 (1):85-93.

8. Moffat BA, Chenevert TL, Hall DE et al. (2005) Continuous arterial spin labeling using a train of adiabatic inversion pulses. J Magn Reson Imaging 21 (3):290-296.

9. Mildner T, Trampel R, Moller HE et al. (2003) Functional perfusion imaging using continuous arterial spin labeling with separate labeling and imaging coils at 3 T. Magn Reson Med 49 (5):791-795.

10. Restom K, Behzadi Y, Liu TT (2006) Physiological noise reduction for arterial spin labeling functional MRI. Neuroimage 31 (3):1104-1115.

11. St Lawrence KS, Frank JA, Bandettini PA et al. (2005) Noise reduction in multi-slice arterial spin tagging imaging. Magn Reson Med 53 (3):735-738.

12. Talagala SL, Ye FQ, Ledden PJ et al. (2004) Whole-brain 3D perfusion MRI at 3.0 T using CASL with a separate labeling coil. Magn Reson Med 52 (1):131-140.

13. Wang J, Licht DJ (2006) Pediatric perfusion MR imaging using arterial spin labeling. Neuroimaging Clin N Am 16 (3):149-167, ix.

14. Wolf RL, Detre JA (2007) Clinical neuroimaging using arterial spin-labeled perfusion magnetic resonance imaging. Neurotherapeutics 4 (3):346-359.

15. Wong EC, Luh WM, Liu TT (2000) Turbo ASL: arterial spin labeling with higher SNR and temporal resolution. Magn Reson Med 44 (4):511-515.

16. Ye FQ, Frank JA, Weinberger DR et al. (2000) Noise reduction in 3D perfusion imaging by attenuating the static signal in arterial spin tagging (ASSIST). Magn Reson Med 44 (1):92-100.

17. Ye FQ, Mattay VS, Jezzard P et al. (1997) Correction for vascular artifacts in cerebral blood flow values measured by using arterial spin tagging techniques. Magn Reson Med 37 (2):226-235.

18. Calamante F, Williams SR, van Bruggen N et al (1996) A model for quantification of perfusion in pulsed labelling techniques. NMR Biomed 9 (2):79-83.

Appendix

To derive an expression for the signal difference between control and labeled spins, we begin with the Bloch equation for longitudinal magnetization of brain tissue water corrected for the effects of arterial and venous flow:

$$\frac{dM(t)}{dt} = -\frac{M_0 - M(t)}{T_1} + fM_a(t) - \frac{f}{\lambda}M(t)\,. \quad [5]$$

Because the perfusion signal is obtained by subtracting two images acquired with arterial spin tagging states but with identical blood flow, the signal from each compartment is defined as the difference in magnetization in i-th interval between the labeled and control scans:

$$ASL\ Signal\colon\ \Delta S_i(t) = M^{control}(t) - M^{label}(t)\,. [6]$$

The difference in magnetization of arterial blood between control and labeled states can be expressed as follows:

$$\frac{(M^{control}(\mathrm{t})-M^{label}(\mathrm{t}))}{dt} =$$

$$-\frac{\left(M^{control}(\mathrm{t})-M^{label}(\mathrm{t})\right)}{T_1} + f\left(M_a^{control}(\mathrm{t}) - M_a^{label}(\mathrm{t})\right) - \frac{f}{\lambda}(M^{control}(\mathrm{t}) - M^{label}(\mathrm{t})). \quad [7]$$

First, z-magnetization of the 1st period is considered as:

$$\frac{\Delta S_1(t)}{dt} = -\frac{\Delta S_1(t)}{T_1} + f\left(M_a^{control}(\mathrm{t}) - M_a^{label}(\mathrm{t})\right) - \frac{f}{\lambda}\Delta S_1(t), \qquad [8]$$

where $T_{1\mathrm{app}}$ is given by

$$\frac{1}{T_{1app}} = \frac{1}{T_1} + \frac{f}{\lambda}, \qquad [9]$$

and the inflowing spins in acquisition of the 1st interval are written as follows:

$$M_a^{control}(\mathrm{t}) = M_{a,1}^0, \quad M_a^{label}(\mathrm{t}) = M_{a,1}^0\left(1 - 2\alpha \mathrm{e}^{-\left(\frac{\mathrm{t}}{\mathrm{T_{1a}}} + \frac{\delta_\mathrm{a}}{\mathrm{T_{1a}}}\right)}\right) \quad (\delta_\mathrm{a} \le t < IT), \qquad [10, 11]$$

where δ_a represents transit time (delay time), and we assume that the label duration (labeling slab width / flow velocity) equals IT.

Then, by substituting Eqs. 9, 10, 11 into Eq. 8, we obtain the following:

$$\frac{\Delta S_1(t)}{dt} + \frac{\Delta S_1(t)}{T_{1app}} = \mathrm{f}(M_a^0 - M_{a,1}^0\left(1 - 2\alpha \mathrm{e}^{-\left(\frac{\mathrm{t}}{\mathrm{T_{1a}}} + \frac{\delta_a}{\mathrm{T_{1a}}}\right)}\right)). \qquad [12]$$

$$\text{where,} \qquad M_a^0 = \frac{M_0}{\lambda}.$$

By substituting this equation into Eq. 12, we obtain the following:

$$\frac{\Delta S_1(t)}{dt} + \frac{\Delta S_1(t)}{T_{1app}} = \frac{2\alpha f M_0}{\lambda} \cdot \mathrm{e}^{-\left(\frac{\mathrm{t}}{T\mathrm{1a}} + \frac{\delta_a}{T1a}\right)} \qquad (\delta_a < t). \qquad [13]$$

Then, the general solution is as follows:

$$\Delta S_1(t) = \mathrm{e}^{-\frac{\mathrm{t}-\delta_a}{T_{1app}}}\left[\frac{2\alpha f M_0}{\lambda}\cdot \mathrm{e}^{-\frac{\delta_a}{T_{1a}}}\cdot\frac{1}{\frac{1}{T_{1app}}-\frac{1}{T_{1a}}}\cdot \mathrm{e}^{\left(\frac{1}{T_{1app}}-\frac{1}{T_{1a}}\right)(\mathrm{t}-\delta_a)} + M + C_1\right]. \qquad [14]$$

where M and C_1 represent initial value of z-magnetization and arbitrary constant in the 1st period, respectively.

Where $S_1(t = 0)$ equal 0, then:

$$C_1 = -\frac{2\alpha f M_0}{\lambda}\cdot e^{-\frac{\delta_a}{T_{1a}}}\cdot\frac{1}{\frac{1}{T_{1app}}-\frac{1}{T_{1a}}}\ . \qquad [15]$$

When we substitute C_1 into the general solution, we obtain the following:

$$\Delta S_1(t) = e^{-\frac{\mathrm{t}-\delta_a}{T_{1app}}}\left[\frac{2\alpha f M_0}{\lambda}\cdot e^{-\frac{\delta_a}{T_{1a}}}\cdot\frac{1}{\frac{1}{T_{1app}}-\frac{1}{T_{1a}}}\cdot \mathrm{e}^{\left(\frac{1}{T_{1app}}-\frac{1}{T_{1a}}\right)(\mathrm{t}-\delta_a)} - \frac{2\alpha f M_0}{\lambda}\cdot e^{-\frac{\delta_a}{T_{1a}}}\cdot\frac{1}{\frac{1}{T_{1app}}-\frac{1}{T_{1a}}}\right]$$

$$(\delta_a < \mathrm{t} \le IT). \qquad [16]$$

Next, we consider the signal change of z-magnetization in the 2nd interval. If we define the ASL signal with the following equation:

$$ASL\ Signal:\ \Delta S_2(t) = M_a^{label}(t) - M_a^{control}(t)\ . [17]$$

we have to note that the signal is obtained from the opposite subtraction between control and labeled states. Then, we can derive the following equation:

$$\frac{\Delta S_2(t)}{dt} + \frac{\Delta S_2(t)}{T_{1app}} = \mathrm{f}(M_{a,2}^0 - M_{a,2}^0\left(1 - 2\alpha \mathrm{e}^{-\left(\frac{\mathrm{t}}{\mathrm{T1a}}+\frac{\delta_a}{\mathrm{T1a}}\right)}\right)) \quad [18]$$

This formula is identical to the equation [12]. The arterial inflow spins are also inverted in the

2nd period after 180 pulse as follows:

$$M^{control}(\mathrm{t}) = M^0_{a,2}\left(1 - 2\alpha \mathrm{e}^{-\frac{\mathrm{t+IT}}{\mathrm{T1a}}}\right),\ M^{label}(\mathrm{t}) = M^0_{a,2} \qquad (IT < t \leq 2IT) \quad [19]$$

Therefore, from the equation [18] and [19], we can obtain the same differential equation as that seen for the 1st period.

$$\frac{\Delta S_2(t)}{dt} + \frac{\Delta S_2(t)}{T_{1app}} = \frac{2\alpha f M_0}{\lambda} \cdot \mathrm{e}^{-\left(\frac{\mathrm{t}}{\mathrm{T1a}} + \frac{\delta_a}{\mathrm{T1a}}\right)} \qquad (IT < t \leq 2IT). \qquad [20]$$

Since the signal of end of the 1st period should be same as the initial signal of the 2nd period, the relationship: S_2(t = IT) = S_1(t = IT) is used.

$$\Delta S_2(t - IT) = \left[\frac{2\alpha f M_0}{\lambda} \cdot \mathrm{e}^{-\frac{\delta_a}{T_{1a}}} \cdot \frac{1}{\frac{1}{T_{1app}} - \frac{1}{T_{1a}}} + S_1(IT) + C_2\right] = S_1(IT). \quad [21]$$

where C_2 represents the arbitrary constant in the 2nd period.

$$C_2 = -\frac{2\alpha f M_0}{\lambda} \cdot e^{-\frac{\delta_a}{T_{1a}}} \cdot \frac{1}{\frac{1}{T_{1app}} - \frac{1}{T_{1a}}}. \quad [22]$$

Therefore,

$$\Delta S_2(t) = e^{-\frac{\mathrm{t}-\delta_a}{T_{1app}}}\left[\frac{2\alpha f M_0}{\lambda} \cdot e^{-\frac{\delta_a}{T_{1a}}} \cdot \frac{1}{\frac{1}{T_{1app}} - \frac{1}{T_{1a}}} \cdot \mathrm{e}^{\left(\frac{1}{T_{1app}} - \frac{1}{T_{1a}}\right)(\mathrm{t}-\delta_a)} + S_1(IT) - \frac{2\alpha f M_0}{\lambda} \cdot e^{-\frac{\delta_a}{T_{1a}}} \cdot \frac{1}{\frac{1}{T_{1app}} - \frac{1}{T_{1a}}}\right]. \quad [23]$$

The signal of the 3rd period can be considered with the same equation used the first period, but with a different start signal, where S_3(t = 2**IT*) = S_2(t = 2**IT*). Therefore,

$$\Delta S_3(t - 2 * IT)|_{t=2*IT} = \left[\frac{2\alpha f M_0}{\lambda} \cdot \mathrm{e}^{-\frac{\delta_a}{T_{1a}}} \cdot \frac{1}{\frac{1}{T_{1app}} - \frac{1}{T_{1a}}} + S_2(2IT) + C_3\right] = S_2(2IT). \quad [24]$$

where C_3 represents the arbitrary constant in the 3rd period.

$$C_3 = -\frac{2\alpha f M_0}{\lambda} \cdot e^{-\frac{\delta_a}{T_{1a}}} \cdot \frac{1}{\frac{1}{T_{1app}} - \frac{1}{T_{1a}}}. \quad [25]$$

$$\Delta S_3(t) = e^{-\frac{\mathrm{t}-\delta_a}{T_{1app}}}\left[\frac{2\alpha f M_0}{\lambda}\cdot e^{-\frac{\delta_a}{T_{1a}}}\cdot\frac{1}{\frac{1}{T_{1app}}-\frac{1}{T_{1a}}}\cdot e^{\left(\frac{1}{T_{1app}}-\frac{1}{T_{1a}}\right)(\mathrm{t}-\delta_a)} + S_2(2IT) - \frac{2\alpha f M_0}{\lambda}\cdot e^{-\frac{\delta_a}{T_{1a}}} \cdot\frac{1}{\frac{1}{T_{1app}}-\frac{1}{T_{1a}}}\right]$$

$$(2IT < t \leq 3IT). \quad [26]$$

Finally, we obtained the general solution of the AIRASL signal for *i*-th period as follows:

$$\Delta S_i(t) = e^{-\frac{(\mathrm{t}-\delta_a-(i-1)*IT)}{T_{1app}}}\left[\frac{2\alpha f M_0}{\lambda}\cdot e^{-\frac{\delta_a}{T_{1a}}}\cdot\frac{1}{\frac{1}{T_{1app}}-\frac{1}{T_{1a}}}\cdot e^{\left(\frac{1}{T_{1app}}-\frac{1}{T_{1a}}\right)(\mathrm{t}-\delta_a-(i-1)*IT)} + S_{i-1}\big((i-1)*IT+\delta_a\big) - \frac{2\alpha f M_0}{\lambda}\cdot e^{-\frac{\delta_a}{T_{1a}}}\cdot\frac{1}{\frac{1}{T_{1app}}-\frac{1}{T_{1a}}}\right] \quad (\delta_a < \mathrm{t}). \quad [27]$$

If δ_a = 0 and *i* = 1, this Eq. 27 is in agreement with the general solution of FAIR in a previous report [18].

Figure

Table 1 Definitions and values of parameters used for signal simulation

f (Gray Matter) : 50	blood perfusion	ml blood/min/100 ml tissue	
λ : 0.90	brain: blood partition coefficient of water	ml /mg	
t	time	s	
δ_a: 0.167	delay time (arrival time)	s	
α : 0.89	Inversion efficiency of labeling pulse	fraction of blood water protons inverted	
M	z-magnetization of tissue water	magnetic moment (ml tissue)$^{-1}$	
M_a	z-magnetization of arterial blood	magnetic moment (ml blood)$^{-1}$	
M_0 : 1.0	equilibrium value of M	magnetic moment (ml tissue)$^{-1}$	
T_1	longitudinal relaxation time of brain water	s	
T_{1a}: 1.120 in 1.5T / 1.600 in 3.0T	longitudinal relaxation time of blood	s	
T_{1app} (Gray Matter) : 0.920 in 1.5T/ 1.200 in 3.0T	apparent relaxation time of brain water	s	

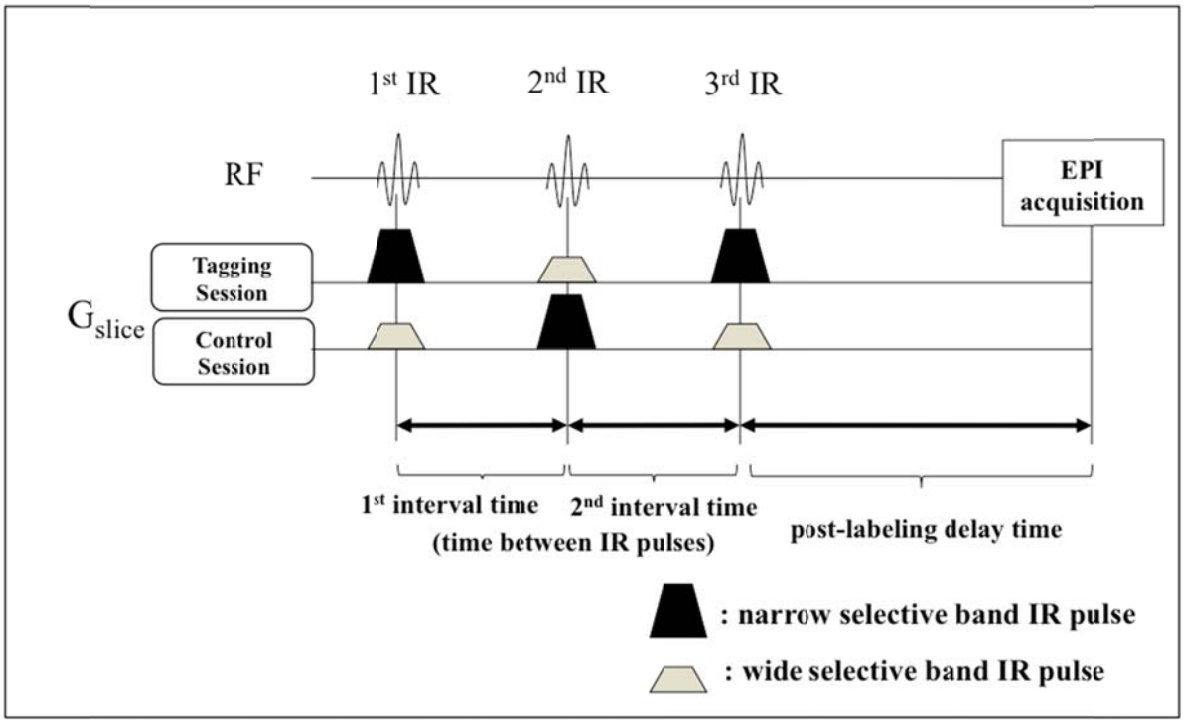

Fig. 1

Fig.1

Pulse sequence diagram for the alternate slab width inversion recovery arterial spin labeling (AIRASL) sequence. Multiple inversion recovery (IR) pulses are used for labeling during echo planar imaging acquisition. In the tagging session, the following spatially selective IR pulse were used: narrow, wide, and narrow, in that order. In the control session, the following spatially selective IR pulse were used: wide, narrow, and wide, in that order.

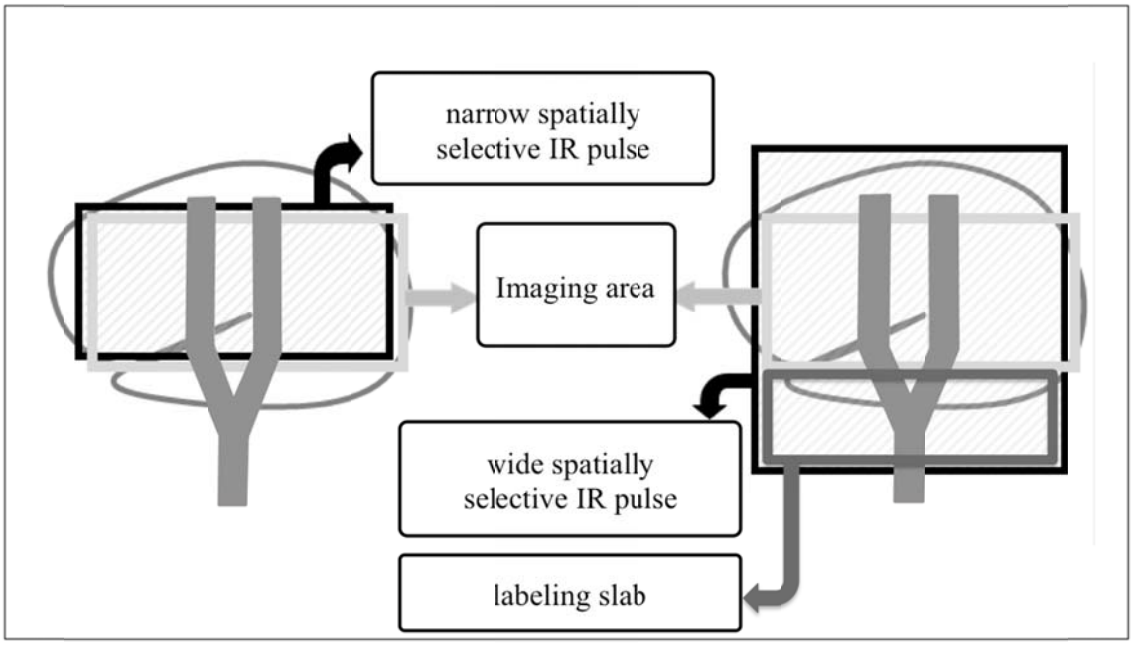

Fig. 2

Fig. 2

Definition of inverted areas for the wide and narrow spatially selective inversion recovery pulses. The labeling slab is the part of the wide slab below the narrow slab.

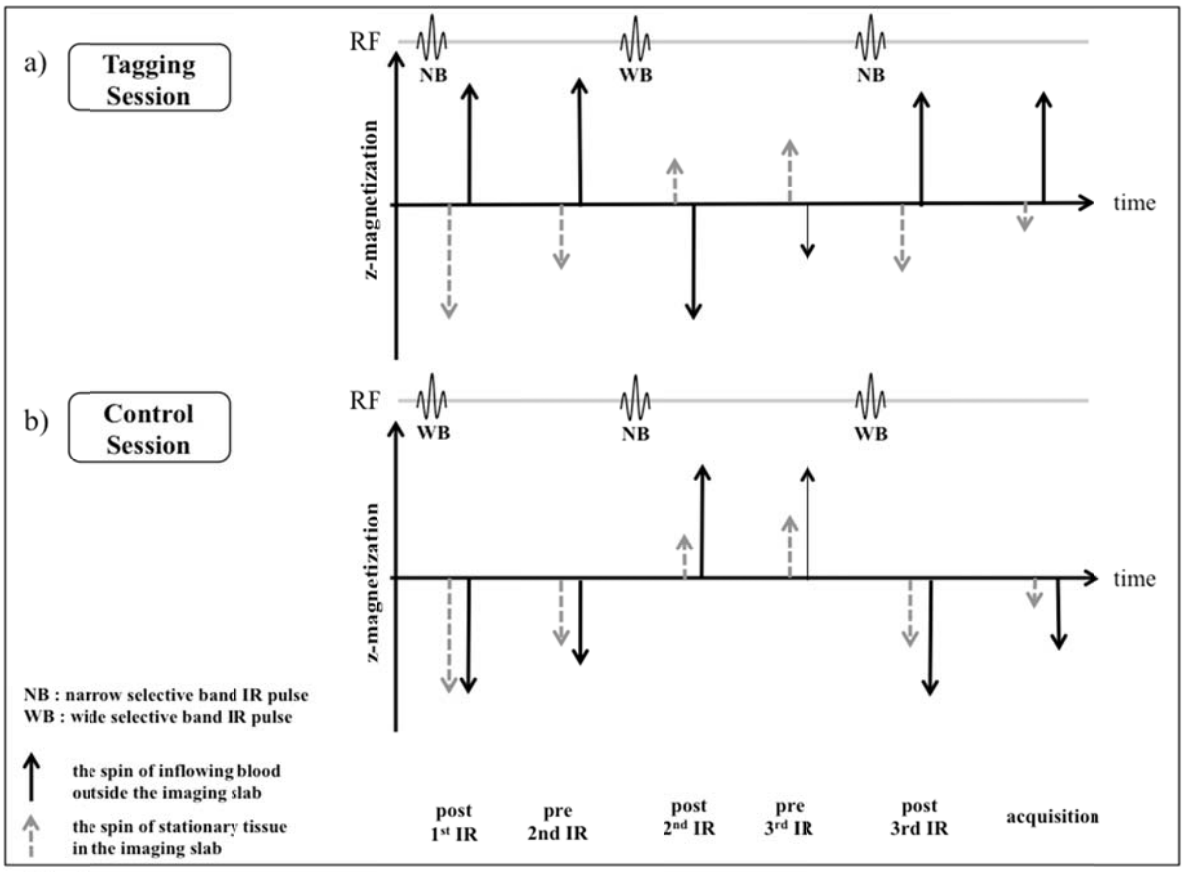

Fig. 3

Fig. 3

Relationship between z-magnetization and the spin of inflowing blood or stationary tissue at each period. (a) In the tagging session, inflowing spins are always opposite to the original spin direction in the imaging slab for each inversion period; thus, a continuous labeling effect can be obtained in the later inversion periods. (b) In the control session, the spins remain in the same direction as the original tissue spins.

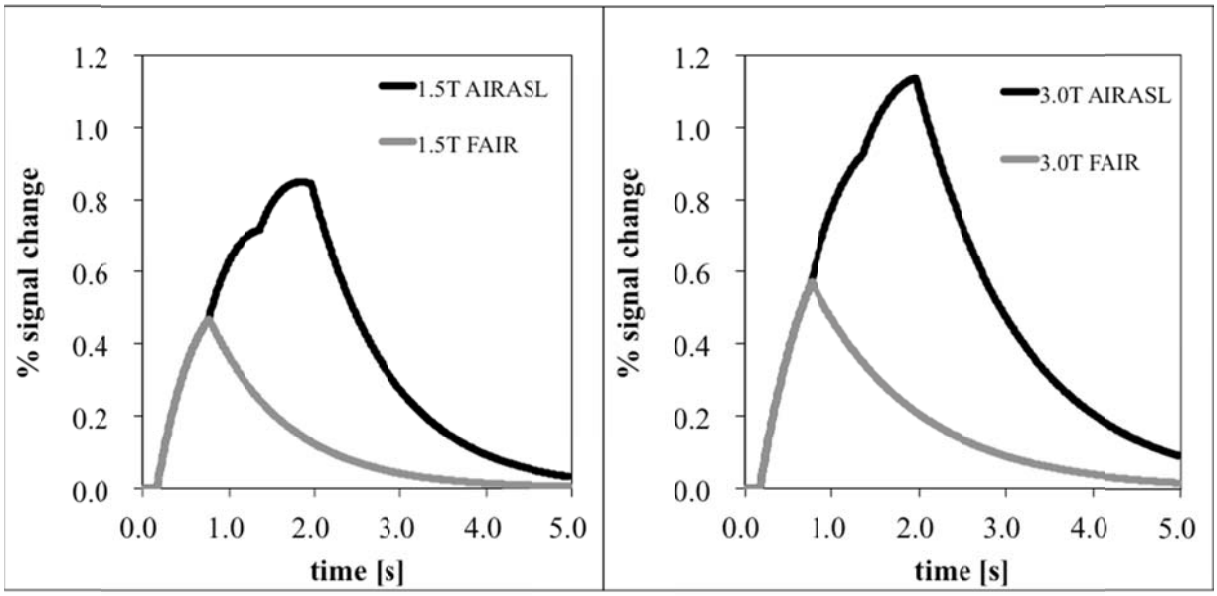

(a) (b)

Fig.4

Fig.4

Simulated percentage difference in signal change, showing passage of the labeled spins through the microvasculature at 1.5T (a) and 3.0T (b). For the distributed solution, the parameters of human gray matter shown in Table 1 used in Eq. 1. The black line shows the difference in signal (i.e., control-labeled) using the AIRASL sequence, and the gray line shows the difference in signal using the flow–sensitive alternating inversion recovery (FAIR) sequence. The signal obtained by AIRASL at 3.0T was 1.14%, whereas the signal obtained by FAIR at 3.0T was 0.57%.

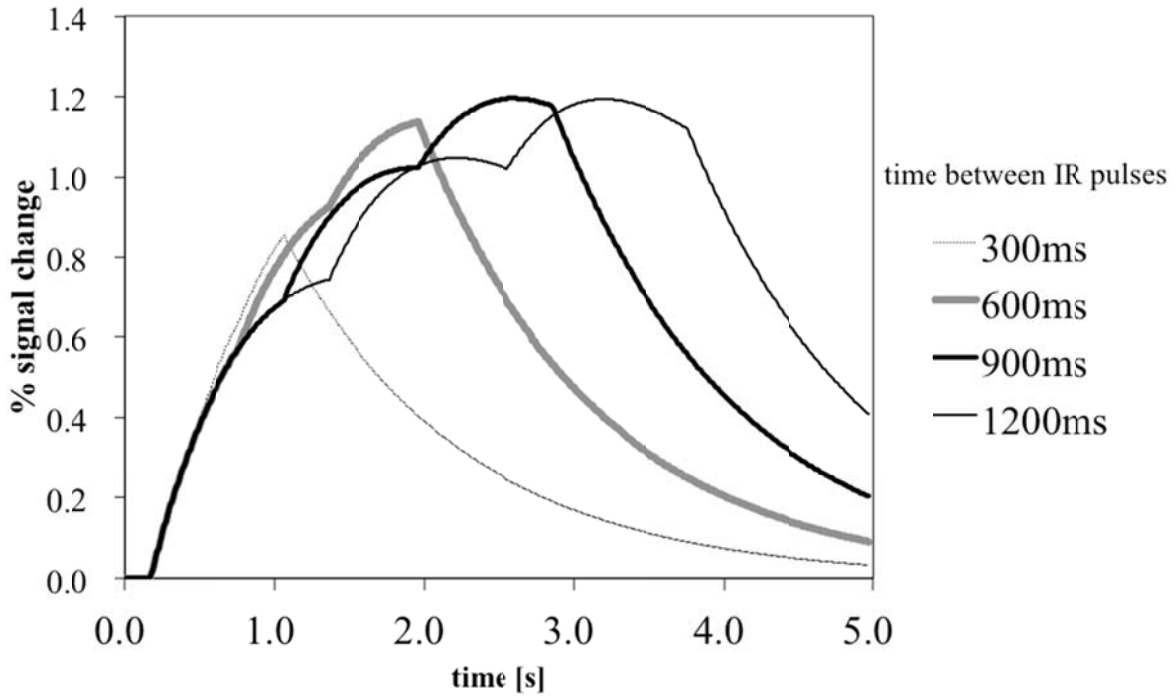

Fig.5

Fig.5

Simulated percentage difference in signal change, showing passage of the labeled spins through the microvasculature using AIRASL with the time between IR pulses (300, 600, 900, 1200 ms) at 3.0T. The optimum setting of the time between IR pulses was 600 ms.

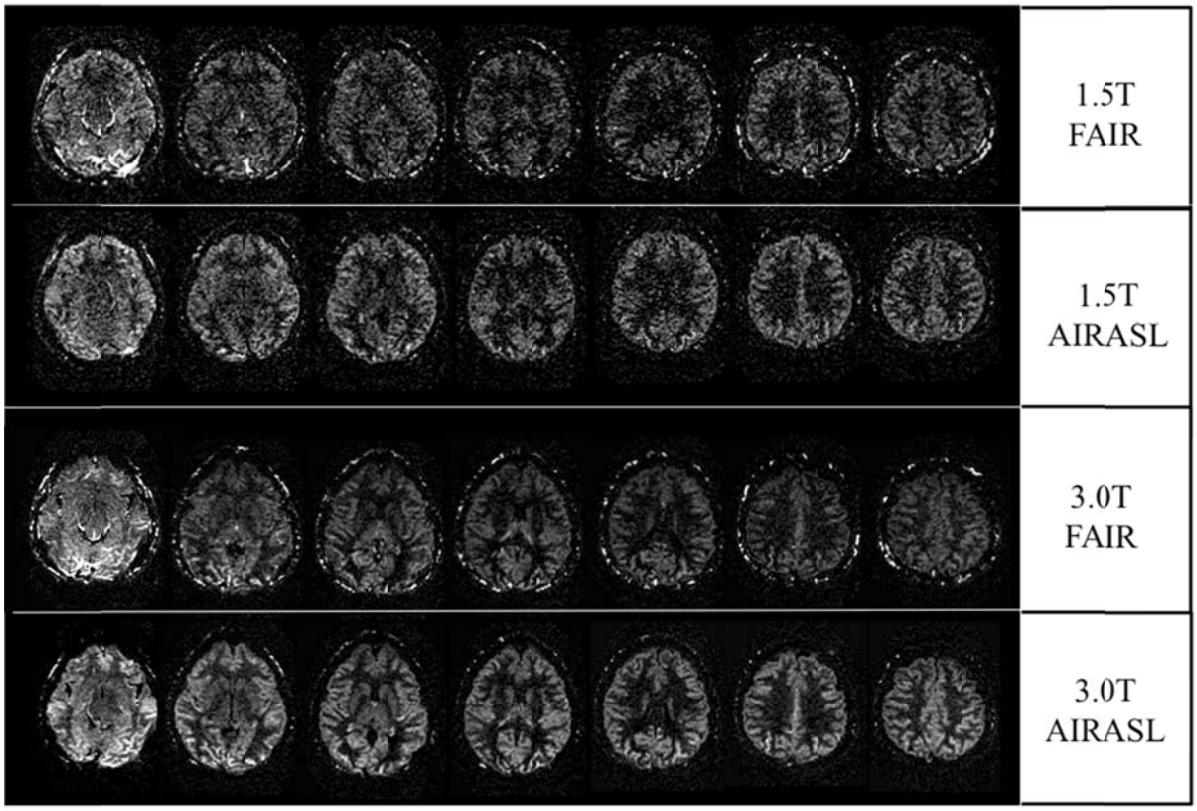

Fig. 6

Fig.6

Comparison of perfusion images acquired by (from top to bottom) 1.5T FAIR, 1.5T AIRASL, 3.0T FAIR, and 3.0T AIRASL for a typical normal subject. Seven slices (6 mm thick, 1 mm interval) from inferior to superior (left to right) cover most of the brain.

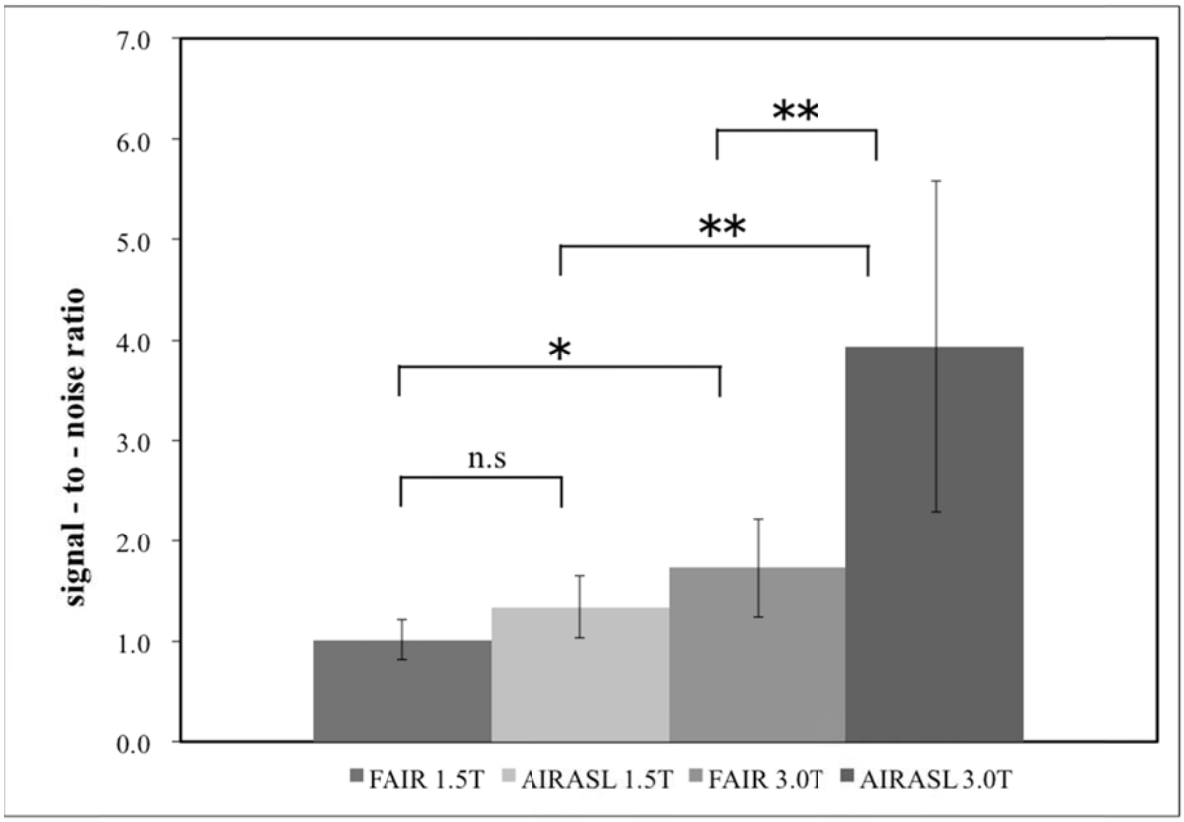

Fig. 7

Fig.7

Image SNR as a function of labeling method and magnetic field strength. The mean SNRs of FAIR (3.0T) and FAIR (1.5T) were 1.73 ± 0.49 and 1.02 ± 0.20, respectively, whereas the SNRs of AIRASL (3.0T) and AIRASL (1.5T) were 3.93 ± 1.65 and 1.34 ± 0.31, respectively. Error bars indicate standard deviation. The result of a paired t-test is shown as n.s. (not significant: $P < .05$), *(significant difference: $P < .05$), or **(significant difference: $P < .01$).